Alexandria Engineering Journal (2022) 61, 4457–4466

HOSTED BY

ELSEVIER

Alexandria University

Alexandria Engineering Journal

www.elsevier.com/locate/aej
www.sciencedirect.com

Investigation of shape effects of Cu-nanoparticle on heat transfer of MHD rotating flow over nonlinear stretching sheet

Tamour Zubair [a], Muhammad Usman [b], Kottakkaran Sooppy Nisar [c,*], Muhammad Hamid [d], Emad E. Mahmoud [e], I.S. Yahia [f,g,h]

[a] *School of Mathematical Sciences, Peking University, Beijing 100871, China*
[b] *Department of Mathematics, National University of Modern Languages (NUML), Islamabad, 44000, Pakistan*
[c] *Department of Mathematics, College of Arts and Sciences, Wadi Aldawaser, 11991, Prince Sattam Bin Abdulaziz University, Saudi Arabia*
[d] *Department of Mechanics and Engineering Sciences, Fudan University, Shanghai 200433, China*
[e] *Department of Mathematics and Statistics, College of Science, Taif University, P.O. Box 11099, Taif 21944, Saudi Arabia*
[f] *Advanced Functional Materials and Optoelectronic Laboratory (AFMOL), Department of Physics, Faculty of Science, King Khalid University, P.O. Box 9004, Abha, Saudi Arabia*
[g] *Research Center for Advanced Materials Science (RCAMS), King Khalid University, P.O. Box 9004, Abha 61413, Saudi Arabia*
[h] *Nanoscience Laboratory for Environmental and Biomedical Applications (NLEBA), Semiconductor Lab, Department of Physics, Faculty of Education, Ain Shams University, Roxy, Cairo 11757, Egypt*

Received 28 July 2021; revised 18 September 2021; accepted 3 October 2021
Available online 20 October 2021

KEYWORDS

Thermal radiation;
Magnetic field;
Stretching surface;
Chebyshev polynomials;
Wavelets;
Grashof number;
Numerical consequence

Abstract In the current study, we focused on the shape effects of copper (Cu) nano-particles on heat transmission of three-dimensional magnetohydrodynamic (MHD) nano-fluid. A particular type of flow is considered, i.e., rotating flow over an exponentially stretching sheet. Significant actions of thermal radiation and Grashof number are also formulated to study. The modified Chebyshev wavelets method is introduced to examine the numerical solutions of the accomplished model. Error analysis and further comparison with existing results reflect the appropriateness of the proposed modification. Graphical behavior of dimensionless velocities, temperature, Nusselt number, and skin friction under the inspiration of several parameters is also presented. The attained solutions propose that the modification is beneficial and can be protracted to other highly nonlinear problems. The modified Chebyshev wavelets technique lowers computing time, according to the study. The research takes into account the form impacts of nano-particles. There are three kinds of nano-particles to examine (spherical, laminar, and cylinder). The behavior of various particles

* Corresponding author.
E-mail addresses: n.sooppy@psau.edu.sa (K.S. Nisar), e.mahmoud@tu.edu.sa (E.E. Mahmoud), isyahia@gmail.com (I.S. Yahia).
Peer review under responsibility of Faculty of Engineering, Alexandria University.

https://doi.org/10.1016/j.aej.2021.10.007

varies depending on the flow and temperature profile. For microparticles with a laminar structure, velocity and temperature have higher values.

1. Introduction

Nowadays, the concept of nano-fluids has become essential and significant for almost every area of science and technology. This is due to the enormous applications of this field of science. It is directly applicable for many areas like in the study of engineering (electronics, industry, printing, devices linked to military) and medical-related sciences (surgery connected with the body, therapy of many dangerous diseases, medicine, food, and nutrition). It has found its applications in the study related to materials and their properties, in the field of computers (in particular, for the computers having unlimited powers), studying the nuclear-based reactor, etc. An overview of the literature related to fluid mechanics exhibits that many theories, laws, and models have been established so far. Basically, nanofluids contain small particles (named nano-particles) in the base of fluids. Due to these specialized particles, fluid properties are altered and adjusted, especially conductivity (thermal) [1] and heat transmission processes. Choi [2] was the first to investigate the improvement of nano-sized particles in fluids. Later, Lee et al. [3] developed the idea of nano-particles and examined the fluid that surrounds the nanotube. Multiple investigators have begun researching in this area due to its numerous applicability in various engineering and sciences applications [4–11] (see Table 1).

Radiative fluids are essentially such a category (of fluids) that yield energy due to radiations settled in the system geometry. This imperative tradition for the circumstance of fluid is significant in countless industrial measures. This category of fluids is exclusively appropriate in those structures in which a particular type of fluid is baptized as "ambient" fluid. Moreover, this research is compelling for several categories of devices in specific areas of space science, which can function at a hefty temperature scale. Frequently, "Stefan approximations" of radiation are applied to different mathematical formulations. Micropolar perceptions, along with radiation enrichment, are offered by Ishak [6]. T. Hayat [12], a renowned mathematician, discussed the unsteady wonders of radiative and magnetic fluid in the same year. Shateyi et al. [13] proposed a method for calculating geometric significances in laminar and radiative flow. Khan [14] et al. put their findings on MHD nano-fluid characteristics and heat energy production perceptions into practice.

Learning MHD procedures and embedding this information on nano-fluid have become very effective and validate for large regions of sciences such as optical modulators and wound behaviors. Moreover, theoretical study of this field provides the knowledge of special forces termed "Lorentz force." This support exists because of the MHD study, which obliges the theme control the chilling (cooling) structures. To model this category of phenomena, the philosophy of Ohm's laws and Maxwell are very significant. The modern thoughts concerning this range can be perceived using these refs. [12–20,22,23,24].

The flow of rotation types is a very significant phenomenon. They are highly functional in numerous areas of science like rotating type of machinery, the flow of magma in the mantle layer of earth, flow of anti-cyclonic, the process of centrifugal filtration, chemical and food procedures, and viscometers. A famous scientist Crane [21], fashioned his important investigation in the arena of flow (stretching). Fuhrer, Wang [22] contributed to study the rotational fluid fashioned by enlarging surface. Further, he cracked this demonstrated problem utilizing perturbation for a slight alteration in parameter k. Afterward, abundant reaches worked on these philosophies and verbalized countless models using rotational fluidic properties. Supplementary concepts can be perceived from specified refs. [23–26,27–48].

The literature review in the preceding paragraphs is only focused on the research of shape impacts of nano-particles on 3D rotating nano-fluid flow across a stretched surface with magnetic field and heat radiation. The numerical results of the proposed modeled physical issue are assessed using the modified Chebyshev wavelets technique, which is a numerical methodology. In the next part of the article, graphical analysis and parametric research are also given to investigate the physical implications of the modeled issue. The proposed method may be tweaked using polynomial and wavelet theory literature analysis.

2. Mathematical and geometrical analysis

Assume three-dimensional rotating and convective free flow of nano-fluid over an elastic sheet occupying $z = 0$ plane. The sheet is continuously stretching with velocity whose components are U_w and V_w in x and y-axis directions, as shown in Fig. 1. Consider the flow is steady, laminar boundary layer, and incompressible. Further, consider the flow rotates with an angular velocity $\Omega = \Omega_0 e^{-(x+y)/L}$, here L and Ω_0 are reference length and average form of velocity, respectively.

Table 1 Thermo-physical properties of blood and nano-particles [11].

Properties	$\beta(\mathrm{K}^{-1})$	$\sigma(\Omega m)$	$c_p(\mathrm{J/kgK})$	$k(\mathrm{W/mK})$	$\rho(\mathrm{kg/m^3})$
Water	21×10^{-5}	0.05	4179	997	0.613
Copper (Cu)	1.67×10^{-5}	5.96×10^{7}	385	8933	401

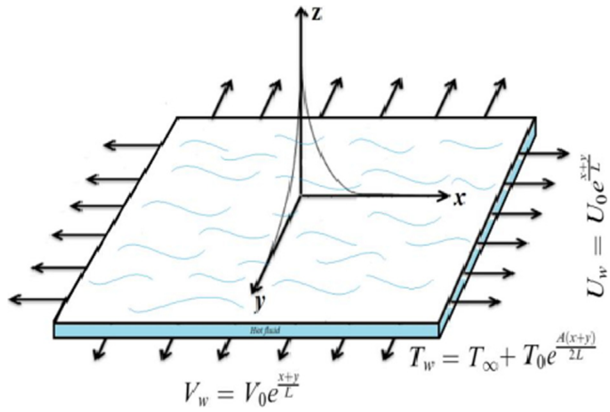

Fig. 1 Systematic diagram of the problem.

A magnetic field of constant nature is applied, and a chemical reaction of the first order is implemented to the system. It is also part of the assumption that all the other sources, such as Joule heating, which affects fluid temperature, are negligibly small. Utilizing the above assumptions, boundary layer approximations, we get the following mathematical model [34]:

$$\frac{\partial u}{\partial x}+\frac{\partial v}{\partial y}+\frac{\partial w}{\partial z}=0, \tag{1}$$

$$u\frac{\partial u}{\partial x}+v\frac{\partial u}{\partial y}+w\frac{\partial u}{\partial z}-2\Omega v=v_{nf}\frac{\partial^2 u}{\partial z^2}+\frac{(\rho\beta)_{nf}}{\rho_{nf}}g(T-T_\infty)-\frac{\sigma_{nf}B_0^2}{\rho_{nf}}u, \tag{2}$$

$$u\frac{\partial v}{\partial x}+v\frac{\partial v}{\partial y}+w\frac{\partial v}{\partial z}-2\Omega u=v_{nf}\frac{\partial^2 v}{\partial z^2}+\frac{(\rho\beta)_{nf}}{\rho_{nf}}g(T-T_\infty)-\frac{\sigma_{nf}B_0^2}{\rho_{nf}}v, \tag{3}$$

$$\frac{(\rho c_p)_{nf}}{(\rho c_p)_f}\left(u\frac{\partial T}{\partial x}+v\frac{\partial T}{\partial y}+w\frac{\partial T}{\partial z}\right)=\frac{k_{nf}}{(\rho c_p)_f}\frac{\partial^2 T}{\partial z^2}+\frac{\mu}{(\rho c_p)_f}\left(\left(\frac{\partial u}{\partial z}\right)^2+\left(\frac{\partial v}{\partial z}\right)^2\right)+\frac{1}{(\rho c_p)_f}\frac{\partial}{\partial z}q_r, \tag{4}$$

The useful relations for nano-particles concepts are explained as [11]:

$$\frac{\mu_{nf}}{\mu_f}=\frac{1}{(1-\phi)^{2.5}},\frac{\rho_{nf}}{\rho_f}=\left(1-\phi+\frac{\rho_s}{\rho_f}\phi\right),$$
$$\frac{\sigma_{nf}}{\sigma_f}=\left(1+\frac{3(\sigma-1)\phi}{(\sigma+2)-(\sigma-1)\phi}\right),$$
$$\frac{(\rho c_p)_{nf}}{(\rho c_p)_f}=\left(1-\phi+\frac{(\rho c_p)_s}{(\rho c_p)_f}\phi\right),$$
$$\frac{(\rho\beta)_{nf}}{(\rho\beta)_f}=\left(1-\phi+\frac{(\rho\beta)_s}{(\rho\beta)_f}\phi\right),$$
$$\frac{k_{nf}}{k_f}=\frac{k_s+(n-1)k_f-(n-1)(k_f-k_s)\phi}{k_s+(n-1)k_f+(k_f-k_s)\phi},\sigma=\frac{\sigma_s}{\sigma_f}.$$

The suitable boundary conditions (BC's) are connected with the above Eqs. (1)–(4) are:

$$u=U_w, v=V_w, w=0, T=T_w, \text{at} z=0, \tag{5}$$

$$u=v=0, T=T_\infty, \text{as} z\to\infty. \tag{6}$$

Further we have:

$$U_w=Ue^{\frac{x+y}{L}}, V_w=Ve^{\frac{x+y}{L}}, T_w=T_\infty+T_0e^{\frac{x+y}{L}}.$$

In above U, V and T_0 are constants, T_∞ is ambient temperature. The last term of Eq. (4) signifies the influence of thermal radiation, which can be written as [11]:

$$\frac{\partial}{\partial z}q_r=-\frac{16}{3}\frac{\sigma^* T_\infty^3}{k^*(\rho c_p)_f}\frac{\partial^2 T}{\partial z^2}.$$

According to the problem, we have the following similarity transformations:

$$\begin{cases} u=Ue^{\frac{x+y}{L}}F'(\varrho), v=Ue^{\frac{x+y}{L}}G'(\varrho), \theta(\varrho)=\frac{T-T_\infty}{T_0}e^{-\frac{A(x+y)}{2L}}, \\ w=-\sqrt{\frac{vU}{2L}}e^{\frac{x+y}{2L}}\left[F(\varrho)+\varrho F'(\varrho)+G(\varrho)+\varrho G'(\varrho)\right], \varrho=z\sqrt{\frac{U}{2vL}}e^{\frac{x+y}{2L}}. \end{cases} \tag{7}$$

We obtained the following set of equations by using the above transformation into the modelled problem (1)–(4):

$$\frac{v_{nf}}{v_f}F'''+F''(F+G)-2F'\left(F'+G'\right)+4\lambda G'+\frac{\rho_f}{\rho_{nf}}\frac{(\rho\beta)_{nf}}{(\rho\beta)_f}Gr\theta=\frac{\rho_f}{\rho_{nf}}\frac{\sigma_{nf}}{\sigma_f}Ha^2F', \tag{8}$$

$$\frac{v_{nf}}{v_f}G'''+G''(F+G)-2G'\left(F'+G'\right)-4\lambda F'+\frac{\rho_f}{\rho_{nf}}\frac{(\rho\beta)_{nf}}{(\rho\beta)_f}Gr\theta=\frac{\rho_f}{\rho_{nf}}\frac{\sigma_{nf}}{\sigma_f}Ha^2G', \tag{9}$$

$$\frac{1}{\Pr}\left(\frac{k_{nf}}{k_f}+Rd\right)\theta''+\frac{(\rho c_p)_{nf}}{(\rho c_p)_f}\left((F+G)\theta'-A\left(F'+G'\right)\theta\right)+Ec_xEc_y\left(F''^2+G'^2\right)=0. \tag{10}$$

Boundary condition gets reduces to as:

$$\begin{cases} f(\varrho)=g(\varrho)=0, f'(\varrho)=1, g'(\varrho)=\alpha, \theta(\varrho)=1, at\varrho=0, \\ f'(\varrho)=g'(\varrho)=0, \theta(\varrho)=0, as\varrho\to\infty. \end{cases} \tag{11}$$

Important symbols and expressions are given in Table 2.

3. Wavelets and Chebyshev wavelets

The third kind Chebyshev wavelets (TKCW) with the influences k,p,j,M defined in [0,1] is given as below [35,36]:

$$\psi_{p,j}(\varrho)=\begin{cases} 2^{\frac{k}{2}}V_j(2^k\varrho-(2p-1)), \frac{p-1}{2^{k-1}}\le\varrho\le\frac{p}{2^{k-1}}, \\ 0 otherwise, \end{cases}$$

where $V_j(\varrho)=\frac{1}{\sqrt{\pi}}V_j(\varrho)$ is represents the j-th-order Chebyshev wavelets. Also $j=0,1,\cdots,M-1, p=0,1,\cdots,2^{k-1}$. The recurrence relation of Chebyshev polynomials of the third kind are explained as:

$$V_0(\varrho)=1, V_1(\varrho)=2\varrho-1, V_j(\varrho)=2\varrho V_{j-1}(\varrho)-V_{j-2}(\varrho), j\ge 2.$$

The weight function Ξ_p of Chebyshev wavelets are give below:

Table 2 Explanation of symbols & expressions (nomenclature).

Name	Symbols&Expressions	Name	Symbols&Expressions
Kinematicviscosity	v	Thermal conductivity	k
Subscriptfornano – fluid	nf	Thermal expansion	β
Electricalconductivity	σ	Mass diffusion	D
Density	ρ	Concentration susceptibility	c_s
Magneticfieldcomponent	B_0	Thermal diffusion ratio	k_T
Temperature	T	Shapefactor	n
Heatcapacity	c_p	Volumefraction	ϕ
Subscriptforbasefluid	f	Eckertnumbersinx	$c_x = \frac{v_f}{\alpha c_p} \frac{U^2}{T_0} \mathrm{e}^{\frac{2x}{L} - \frac{Ax}{2L}}$
Rotation	$\lambda = \frac{\Omega L}{U} \mathrm{e}^{-\frac{x+y}{L}}$	Eckertnumbersiny	$Ec_y = \frac{v_f}{\alpha c_p} \frac{U^2}{T_0} \mathrm{e}^{\frac{2y}{L} - \frac{Ay}{2L}}$
Hartmannnumber	$Ha^2 = \frac{2\sigma_f L B_0^2}{U\rho} \mathrm{e}^{-\frac{x+y}{L}}$	Stretchingratio	$\alpha = \frac{V}{U}$
Grashofnumber	$Gr = \frac{2L\beta_f g T_0}{U^2} \mathrm{e}^{\frac{A(x+y)}{2L} - \frac{2(x+y)}{L}}$	Radiation	$Rd = \frac{16\sigma^* T_\infty^3}{3k^* k_f}$
Prandtlnumber	$\Pr = \frac{k_f}{v_f \left(\rho c_p\right)_f}$	Skin Friction in$x$	$\sqrt{\frac{\mathrm{Re}_x}{2}} C_{fx} = -\mathrm{e}^{\frac{3(x+y)}{2L}} \frac{\rho_f}{\rho_{nf}} \frac{\mu_{nf}}{\mu_f} F''(0)$
Nusselt number	$\frac{\sqrt{2}L}{x} \frac{Nu_x}{\sqrt{\mathrm{Re}_x}} = -\left(\frac{k_{nf}}{k_f} + Rd\right) \mathrm{e}^{\frac{x+y}{2L}} \theta'(0)$	Skin Friction in$y$	$\sqrt{\frac{\mathrm{Re}_x}{2}} C_{fy} = -\mathrm{e}^{\frac{3(x+y)}{2L}} \frac{\rho_f}{\rho_{nf}} \frac{\mu_{nf}}{\mu_f} G''(0)$
Reynolds number	$Re = \frac{UL}{v}$	Angular velocity	$\Omega = \Omega_0 \mathrm{e}^{-(x+y)/L}$

$$\Xi_p(\varrho) = \Xi\left(2^k \varrho - (2p_1 - 1)\right) = \sqrt{\frac{1 + (2^\kappa \varrho - (2p - 1))}{1 - (2^\kappa \varrho - (2p - 1))}}.$$

With the concepts of TKCW, we can write as:

$$F(\varrho)\big|_{L^2(\mathbb{R}),[0,1)} = \sum_{p=1}^{\infty} \sum_{j=0}^{\infty} \xi_{p,j} \psi_{p,j}(\varrho)\Big|_{\xi_{pj} = \int_0^1 F(\varrho)\psi_{pq}(\varrho)\Xi_p \mathrm{d}\varrho = \langle F(\varrho), \psi_{p,q}(\varrho)\rangle_{L^2_\Xi[0,1)}}$$

The above-defined equation is truncated as:

$$F(\varrho) = \sum_{p=1}^{2^{\kappa-1}} \sum_{q=0}^{M-1} \xi_{pq} \psi_{pq}(\varrho) = \mathscr{M}^T \psi(\varrho),$$

where $\psi(\varrho)$and $\mathscr{M}$ are specified in [35–38].

4. Solution procedure

This section scrutinizes the methodology and application of the modified Chebyshev wavelets method to find the solution (8–10). This revised version has the following steps:

Step 1. First, consider (8–10):

$$\frac{v_{nf}}{v_f} F''' + F''(F + G) - 2F'\left(F' + G'\right) + 4\lambda G' + \frac{\rho_f}{\rho_{nf}} \frac{(\rho\beta)_{nf}}{(\rho\beta)_f} Gr\theta = \frac{\rho_f}{\rho_{nf}} \frac{\sigma_{nf}}{\sigma_f} Ha^2 F', \tag{12}$$

$$\frac{v_{nf}}{v_f} G''' + G''(F + G) - 2G'\left(F' + G'\right) - 4\lambda F' + \frac{\rho_f}{\rho_{nf}} \frac{(\rho\beta)_{nf}}{(\rho\beta)_f} Gr\theta = \frac{\rho_f}{\rho_{nf}} \frac{\sigma_{nf}}{\sigma_f} Ha^2 G', \tag{13}$$

$$\frac{1}{\Pr}\left(\frac{\kappa_{nf}}{\kappa_f} + Rd\right)\theta'' + \frac{(\rho c_p)_{nf}}{(\rho c_p)_f}\left((F + G)\theta' - A\left(F' + G'\right)\theta\right) + Ec_x Ec_y\left(F''^2 + G'^2\right) = 0. \tag{14}$$

Step 2. The trial solution according to Chebyshev wavelets method for solving Eqs. (12)–(14) are givens as:

$$\mathscr{T}(\aleph) = \mathbf{C}_l^T \psi(\varrho), \tag{15}$$

where $\sum_{i=1}^{2^{k-1}} \sum_{j=0}^{M-1} \Delta_{ij}^q \mathscr{H}_{ij}(\aleph) = \mathbf{C}_l^T \psi(\varrho), q = l = 1, 2, 3$ for $\mathscr{T}(\aleph) = (F(\aleph), G(\aleph), \theta(\aleph))$ respectively.

$$\mathbf{C}_l = \left[\Delta_{1,k}^i\right]^T, k = 0, 1, 2, \cdots$$

The above solution (15) can be rephrased as:

$$\mathscr{T}(\aleph) = \Lambda_l^T \chi(\varrho), \chi(\varrho) = \left[1, \varrho, \varrho^2, \varrho^3, \cdots\right]^T. \tag{16}$$

where $\Lambda_p, p = 1, 2, 3$ are explained in refs. [31,32]. Therefore; we further have

$$\mathscr{T}(\aleph) = \sum_{n=0}^{M} \overset{1}{\zeta}_n \varrho^n. \tag{17}$$

Step 3. After inserting the trial solutions (22–24) into Eqs. (8)–(10), we got the following residuals for velocities and temperature:

$$\mathbf{R}_F = \frac{v_{nf}}{v_f} F''' + F''\left(F + G\right) - 2F'\left(F' + G'\right) + 4\lambda G' + \frac{\rho_f}{\rho_{nf}} \frac{(\rho\beta)_{nf}}{(\rho\beta)_f} Gr\,\theta - \frac{\rho_f}{\rho_{nf}} \frac{\sigma_{nf}}{\sigma_f} Ha^2 F',$$

$$\mathbf{R}_G = \frac{v_{nf}}{v_f} G''' + G''\left(F + G\right) - 2G'\left(F' + G'\right) - 4\lambda F' + \frac{\rho_f}{\rho_{nf}} \frac{(\rho\beta)_{nf}}{(\rho\beta)_f} Gr\,\theta - \frac{\rho_f}{\rho_{nf}} \frac{\sigma_{nf}}{\sigma_f} Ha^2 G',$$

$$\mathbf{R}_\theta = \frac{1}{\Pr}\left(\frac{\kappa_{nf}}{\kappa_f} + Rd\right)\theta'' + \frac{(\rho c_p)_{nf}}{(\rho c_p)_f}\left(\left(F + G\right)\theta' - A\left(F' + G'\right)\theta\right) + Ec_x Ec_y\left(F''^2 + G'^2\right).$$

Step 4. Now Galerkin method is applied in order to analyze the values of ζ's. We have:

$$\mathscr{K}_{\ell}^{n}=\int_{0}^{\varrho_\infty}\mathbf{R}_{\ell}\frac{\mathrm{d}}{\mathrm{d}\tau_{n}^{l}}\ell(\aleph)\mathrm{d}\varrho, n=1,2,\cdots,2^{\kappa-1}M-3,$$

where $\ell=(F,G,\theta)$, $\mathscr{K}_{\ell}^{n}=(\mathbf{E}_{F}^{n},\mathbf{E}_{G}^{n},\mathbf{E}_{\theta}^{n})$, $\mathbf{R}_{\ell}=(\mathbf{R}_{F},\mathbf{R}_{G},\mathbf{R}_{\theta})$ and $l=1,2,3$ for F,G and θ respectively.

Step 5. The values of Δ's (unknowns) is achieved. Consequently, the values of Δ's accomplished by inserting the unknowns Δ's.

5. Results and discussion

To explore the physical features of both parametric and shape effects on velocity and temperature, numerical solution of the expressed model is offered in the earlies section, has been evaluated using a modified version of scheme modified Chebyshev wavelets method. Graphical analysis for shape and parametric effects on physical quantities of interest, temperature, and velocity are presented in Figs. 2–8. Furthermore, results and discussion regarding Figs. 2–8 are also part of this portion of the paper. For simplicity purposes, we consider $\varrho=\eta$.

The "Nusselt number" and "skin friction" are explained in Figs. 2 and 3. It can be seen that skin friction coefficient both x and y-direction demonstrate the growing behavior against the Hartmann number. This energy is added to the system, and further fluid particles are more excited due to it. Therefore, it becomes a significant increase in temperature and velocity. Due to the variation in rotating parameter coefficient (x-directional skin friction) decreases gradually, and the reverse effect of rotating parameter achieved for y-directional "skin friction." It has the dominant values for the case of the sphere shape of the nano-particle. Nusselt number (Nu_x) upsurges due to the changes in Pr, α, and β. Nu_x decrease as enhancing the Ec_x. Similar results of the Nusselt number can be obtained for the Eckert number in y-direction.

Furthermore, Figs. 4–8 are graphical behavior analyses of velocity and temperature for distinct numerical values of parameters. Fig. 4(a) displays the effects of velocity

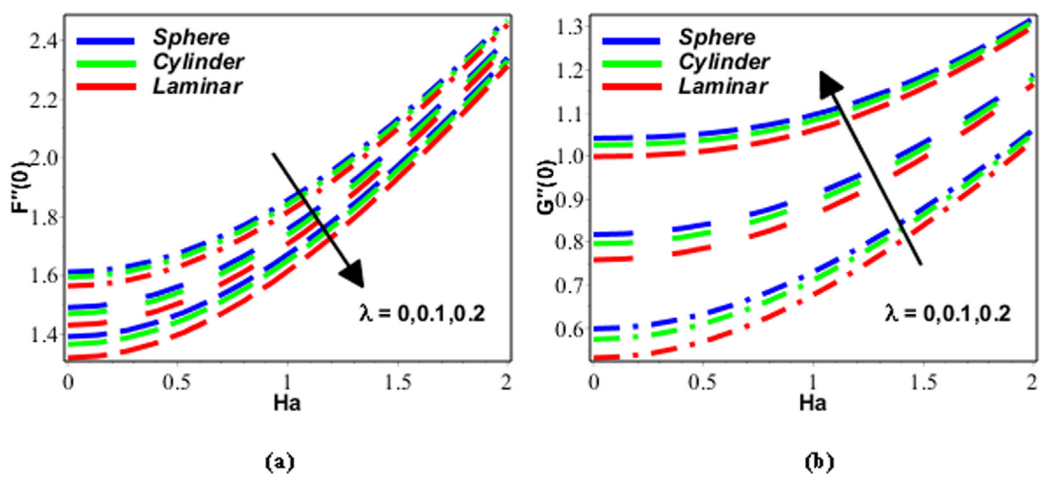

Fig. 2 **(a-b).** The consequence of λ on **(a)** skin friction coefficients C_{fx} **(b)** skin friction coefficients C_{fy}.

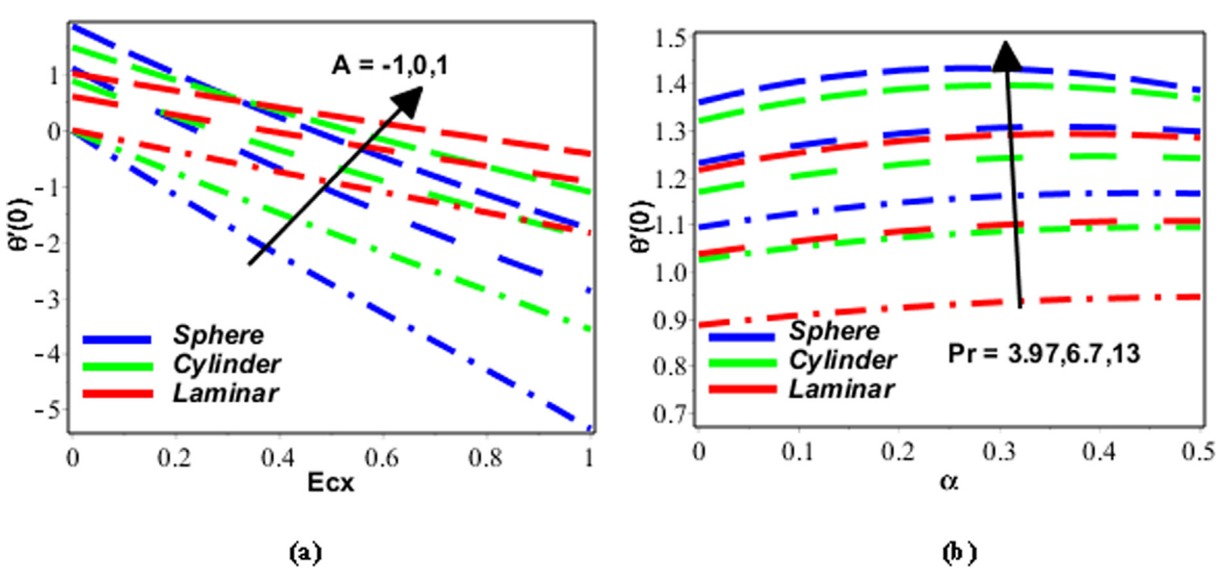

Fig. 3 **(a-b).** **(a)** The consequence of A on Nusselt number (Nu_x) **(b)** Effect of Pr on Nusselt number (Nu_x).

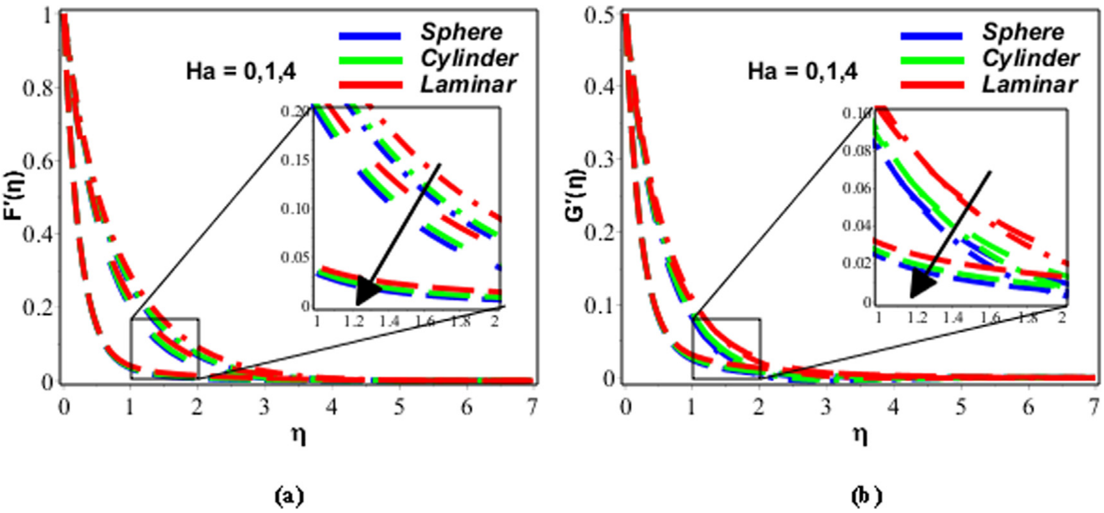

Fig. 4 **(a-b).** Consequence of Ha on **(a)** velocity in x-direction **(b)** velocity in y-direction when $\lambda = 0.1, \phi = 0.1, Gr = 0.9, \alpha = 0.5$.

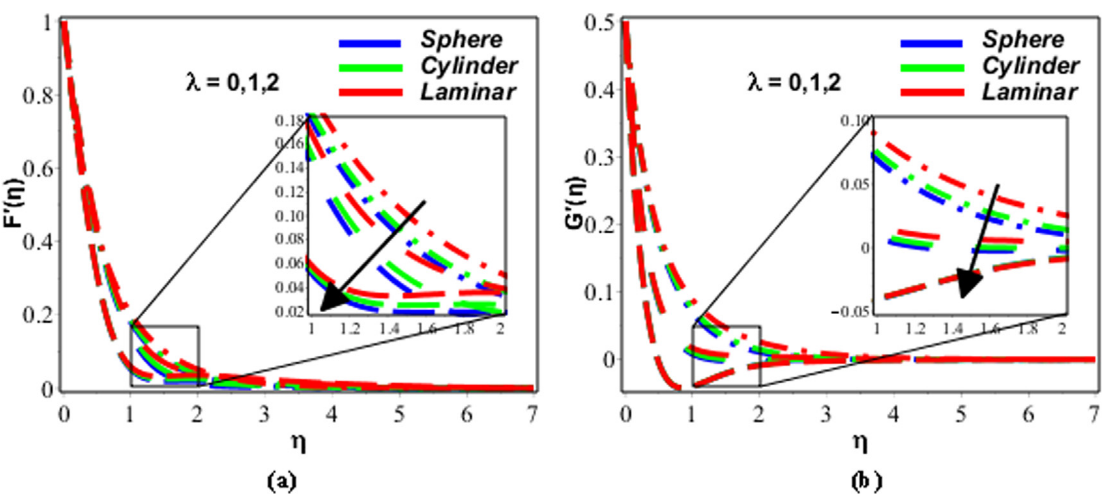

Fig. 5 **(a-b).** Result of λ on **(a)** velocity in x-direction **(b)** velocity in y-direction when $Ha = 2, \phi = 0.1, Gr = 0.9, \alpha = 0.5$.

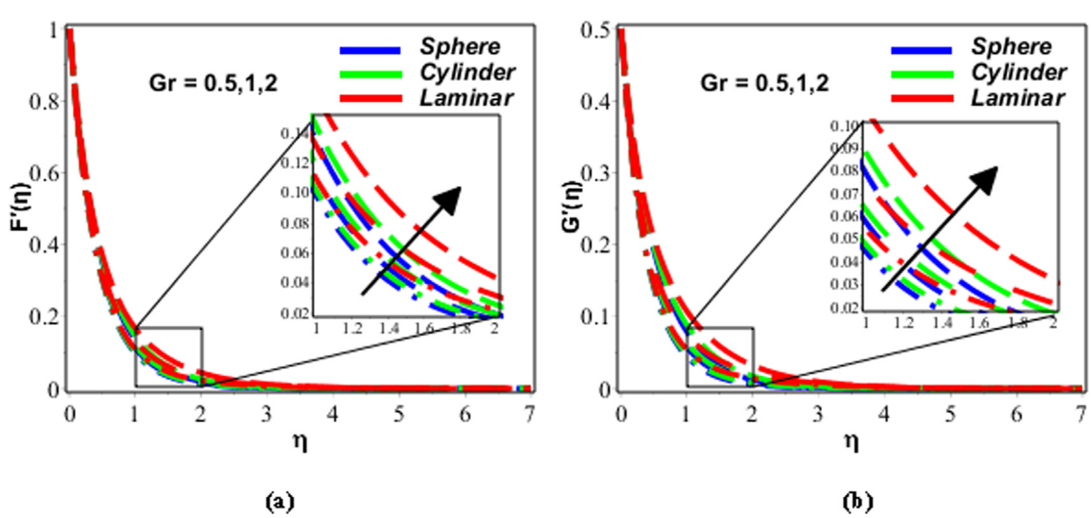

Fig. 6 **(a-b).** Outcome of Gr on **(a)** velocity in x-direction **(b)** velocity in y-direction when $Ha = 2, \lambda = 0.1, \phi = 0.1, \alpha = 0.5$.

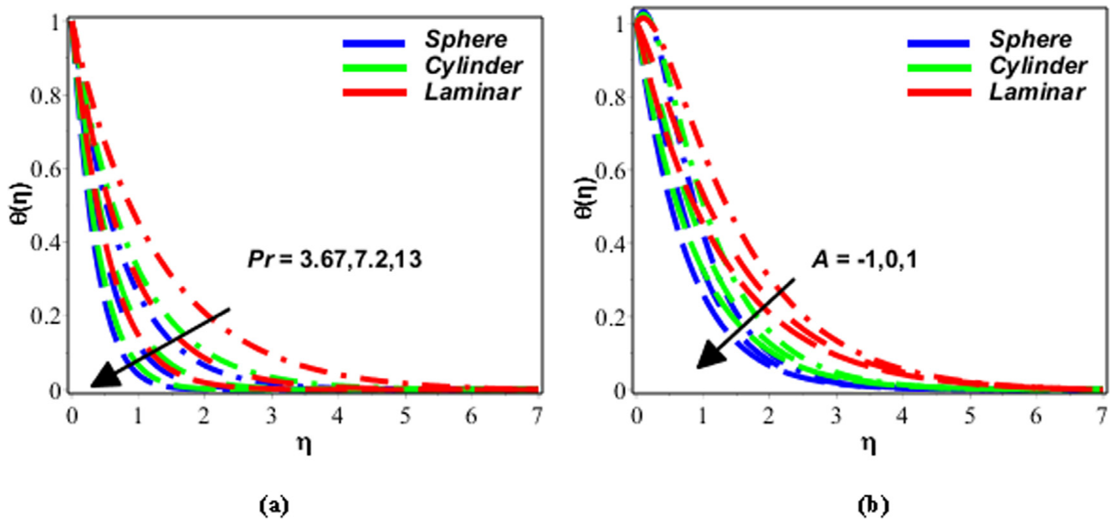

Fig. 7 **(a-b).** Outcome of **(a)** Pr on tempertaure for $Ha = 2, \lambda = 0.9, \phi = 0.1, Gr = 0.9, \alpha = 0.5, Rd = 0.5, Ec_y = 0.5, Ec_x = 0.5, A = 0.9$ **(b)** A on tempertaure for $Ha = 2, \lambda = 0.9, \phi = 0.1, Gr = 0.9, Rd = 0.5, Ec_y = 0.5, Pr = 3.97, Ec_x = 0.3$.

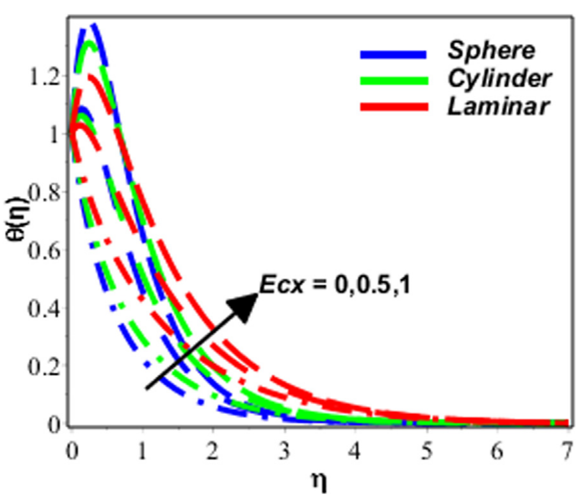

Fig. 8 Consequence of Ec_x on tempertaure for $Ha = 2, \lambda = 0.9, \phi = 0.1, Gr = 0.9, \alpha = 0.5, Rd = 0.5, Ec_y = 0.5, Pr = 3.97, A = 0.9$.

($x-$component) concerning aggregating numerical values of parameter Hartman number is presented. Fig. 4(a) elucidate that the velocity component of the system is lessening with cumulative values of Ha^2. With the help of the physical study of Hartman number, we can easily claim that this parameter exists because of the noteworthy magnetic field, which plays the role of an opponent of the fluid to flow. Due to this opposition regarding the flow of fluid, the fluidic velocity is gradually decreasing. Similar effects are observed in Fig. 4(b) for $y-$component of velocity. On the other hand, velocity due to the laminar particle is high compared to other particles like spherical and cylindrical shapes. In the subsequent Fig. 5(a-b), effects of velocity (x and $y-$components) due to variated values of rotation parameter are offered, and observations show that velocity is lessening concerning rotation parameter, which is growing. That is why increasing rotation effects have produced the disturbance in the flow of fluid, and hence velocity is increased. On the other side, in comparison between Fig. 4(a-b) and 5(a-b), similar effects regarding the shape of the particles are observed. In Fig. 6(a-d), the performance of velocity with altered Gr is categorized. Grashof number is reinforced to boost the nano-fluid velocity.

For the sake of observations regarding temperature, Figs. 7 and 8 are strategized. In Fig. 7(a), the declining effects of temperature with increasing values Prandtl number are explained graphically. In the view of physical aspects of Prandtl number, this can easily understand that thermal diffusion of the nanofluid and Prandtl number is connected with a specific relation named inversely proportional relation. Due to this particular reason, the temperature of the system (based on nanoparticles) is increased. In the next, Fig. 7(b) is explained the decreasing effects of temperature due to the enhancement of the temperature exponent parameter. Fig. 8 is strategized to

Table 3 Different Shapes of nano-particles [29–35].

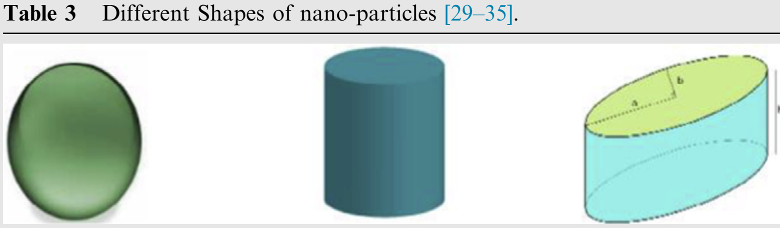

Sphere (m = 3)	Cylinder (m = 6.3698)	Laminar (m = 16.1576)

Table 4 Comparison of the skin friction values achieved from MCWM with available results in the literature.

		$\theta'(0)$		
Pr	A	[38]	[34]	Obtained results
1	1.5	0.377413	0.37741256	0.37741345
	0	0.549643	0.54964375	0.54964377
	1	0.954782	0.95478270	0.95478269
	3	1.560294	1.56029540	1.56029542
5	1.5	1.353240	1.35324050	1.35324049
	0	1.521243	1.52123900	1.52123898
	1	2.500135	2.50013157	2.50013155
	3	3.886555	3.88655510	3.88655507
10	1.5	2.200000	2.20002816	2.20002819
	0	2.257429	2.25742372	2.25742373
	1	3.660379	3.66037218	3.66037222
	3	5.635369	5.62819631	5.62819628

enlighten the arrogance of temperature for growing numerical values of Ec_x. The increasing attitude of temperature in the presented Fig. 8, is due to the directly proportional relation between Eckhart number and viscosity of the fluid. Increase in temperature is also due that Ec_x is the coefficient of viscous dissipation, which corresponsive the enhancement of heat dissipations due to some friction forces. As a result, a certain amount of heat energy is added to the fluid. The change in shape also affects the temperature of the fluid, which can be seen in the Fig. 8 (see Table 3).

Table 4 is presented to assess the important factor "skin friction" accomplished from MCWM with the currently available scheme in refs. [29,33]. Numerical results show the accuracy and compatibility of the suggested scheme. Residual error offered in Table 5 whose expressions are given below as:

Table 5 Residual error for dissimilar order of estimates.

Order of approximation	∇_F	∇_G	∇_θ
4	1.0141×10^{-04}	3.0471×10^{-03}	3.6187×10^{-05}
7	2.1540×10^{-13}	4.1004×10^{-10}	3.0556×10^{-12}
12	3.6540×10^{-20}	5.1140×10^{-18}	1.5470×10^{-18}
17	5.0115×10^{-22}	3.1120×10^{-22}	5.0580×10^{-23}
21	4.7781×10^{-33}	3.2512×10^{-31}	1.5820×10^{-33}

$$\nabla_F = \int_0^{\varrho_\infty} \left[\frac{\nu_{nf}}{\nu_f} F''' + F''\left(F+G\right) - 2F'\left(F' + G'\right) + 4\lambda G' + \frac{\rho_f}{\rho_{nf}} \frac{(\rho\beta)_{nf}}{(\rho\beta)_f} Gr\,\theta - \frac{\rho_f}{\rho_{nf}} \frac{\sigma_{nf}}{\sigma_f} Ha^2 F' \right]^2 d\varrho,$$

$$\nabla_G = \int_0^{\varrho_\infty} \left[\frac{\nu_{nf}}{\nu_f} G''' + G''\left(F+G\right) - 2G'\left(F' + G'\right) - 4\lambda F' + \frac{\rho_f}{\rho_{nf}} \frac{(\rho\beta)_{nf}}{(\rho\beta)_f} Gr\,\theta - \frac{\rho_f}{\rho_{nf}} \frac{\sigma_{nf}}{\sigma_f} Ha^2 G' \right]^2 d\varrho,$$

$$\nabla_\theta = \int_0^{\varrho_\infty} \left[\frac{1}{\Pr}\left(\frac{\kappa_{nf}}{\kappa_f} + Rd\right)\theta'' + \frac{(\rho c_p)_{nf}}{(\rho c_p)_f}\left(\left(F+G\right)\theta' - A\left(F' + G'\right)\theta\right) + Ec_x Ec_y \left(F''^2 + G'^2\right) \right]^2 d\varrho.$$

It can be observed that error $[\nabla_F, \nabla_G, \nabla_\theta] \to 0$ as enhancing the order of approximations.

6. Conclusion

This report covers both the various ways heat is transferred, as well as forms of $Cu-$nanoparticles, shown here. We use a modified version of the algorithm to provide better results. Also, the consequences of radiation and Gr are touched on in the discussion. As a result, the following conclusions are outlined:

- The modified Chebyshev wavelets technique lowers computing effort and is very efficient in solving problems.
- Nanofluids based on copper oxide nano-particles have slow velocity than the other nano-fluids. This is due to the copper oxide nano-particles, which enhance the viscosity of the nano-fluid over the different nano-fluids. It allows the nano-fluid to take more time on the heated surface and thus absorbs more heat from the surface than other nano-fluids.

- "Skin friction" demonstrates the increasing behavior against the Hartmann number. Due to the variation in rotating parameter, x-directional "skin friction" decreases gradually, and the reverse effect of rotating parameter is achieved for y-directional skin friction coefficient.
- "Skin friction" has the maximum values for the sphere shape of the nano-particle.
- The Nusselt number increases owing to Pr, the stretching ratio parameter, and the temperature exponent parameter and decreases as the Eckert number increases.
- The laminar shape of nano-particles is dominated by velocity and temperature profiles.

Declaration of Competing Interest

The authors declare that they have no known competing financial interests or personal relationships that could have appeared to influence the work reported in this paper.

Acknowledgements

The authors express their appreciation to the Deanship of Scientific Research at King Khalid University for funding this work through research groups program under grant number R.G.P.2/61/40. Emad E. Mahmoud acknowledges Taif University Researchers Supporting Project number (TURSP-2020/20), Taif University, Taif, Saudi Arabia.

References

[1] J.A. Eastman, S.U.S. Choi, S. Li, W. Yu, L.J. Thompson, Anomalously increased effective thermal conductivities of ethylene glycol-based nano-fluids containing copper nano-particles, Appl. Phys. Lett. 78 (6) (2001) 718–720.

[2] S.U.S. Choi, Enhancing thermal conductivity of fluids with nano-particles, ASME fluid Eng. Division 231 (1995) 99–105.

[3] H. Xie, H. Lee, W. Youn, M. Choi, Nanofluids containing multiwalled carbon nanotube and their enhanced thermal conductivities, J. Appl. Phys. 94 (2003) 4967–4971.

[4] D. Nield, A. Kuznetsov, Thermal instability in a porous medium layer saturated by nano-fluid, Int. J. Heat Mass Transfer 52 (2009) 5796–5801.

[5] K. Anoop, T. Sundararajan, S. Das, Effect of particles size on the convective heat transfer in nano-fluid in the developing region, Int. J. Heat Mass Transfer 52 (2009) 2189–2195.

[6] A. Ishak, Thermal boundary layer flow over a stretching sheet in a micropolar fluid with radiation effect, Meccanica 45 (2010) 367–373.

[7] M.A. Raza, Z. Kanwal, A. Rauf, A.N. Sabri, S. Riaz, S. Naseem, Size-and shape-dependent antibacterial studies of silver nano-particles synthesized by wet chemical routes, Nanomaterials. 6 (4) (2016 Apr) 74.

[8] M. Shakhaoath, I. Karim, L. Ershad, A. Islam, Unsteady MHD free convection boundary layer flow of a nano-fluid along a starching sheet with thermal radiation and viscous dissipation effects, Int. Nano Lett. (2012) 2–24.

[9] Z. Wu, S. Yang, W. Wu, Shape control of inorganic nano-particles from solution, Nanoscale. 8 (3) (2016) 1237–1259.

[10] M. Nawaz, T. Zubair, Finite element study of radiative nano-plasma flow subjected to Hall and ion slip current, Res. Phy. 7 (2017) 4111–4122.

[11] B. Ankamwar, Size and shape effect on biomedical applications of nanomaterials, Biomed. Eng.-Tech. Appl. Med. 6 (2012 Sep) 93–114.

[12] T. Hayat, M. Qasim, Z. Abbas, Radiation and mass transfer effects on the magnetohydrodynamic unsteady flow induced by a stretching sheet, Z. Naturforsch., 65a(2010), 231-239.

[13] S. Shateyi, J. Prakash, A new numerical approach for MHD laminar boundary layer flow and heat transfer of nano-fluids over a moving surface in the presence of thermal radiation, Bou. Val. Prob., (2014) 2.

[14] W. Khan, O. Makinde, Z. Khan, Non-aligned MHD stagnation point flow of variable viscosity nano-fluid past a stretching sheet radiative heat, Int J. Heat Mass Transfer 96 (2016) 525–534.

[15] G. Sutton, A. Sherman, Engineering magnetohydrodynamics, Mc Graw Hill (1965).

[16] J.C. Newman Jr, An improved method of collocation for the stress analysis of cracked plates with various shaped boundaries, (1971).

[17] S. Shateyi, G. Tendayi, Numerical analysis of unsteady MHD flow near a stagnation point of a two-dimensional porous body with heat and mass transfer, Thermal radiation and chemical reaction, Bou. Val. Prob. 5 (2014) 218.

[18] T. Hayat, T. Muhammad, A. Qayyum, A. Alsaedi, M. Mustafa, On squeezing flow of nano-fluid in the presence of magnetic field effects, J. Mol. Liquid 213 (2016) 179–185.

[19] Y. Lin, L. Zhang, X. Zhang, L. Ma, G. Chen, MHD pseudo-plastic nano-fluid unsteady flow and heat transfer on the finite thin film on a stretching surface internal heat generation, I, J. Heat Mass Transfer 84 (2015) 903–911.

[20] R. Ul Haq, S. Nadeem, Z.H. Khan, N.F.M. Noor, MHD squeezed flow of water functionalized metallic nano-particles over a sensor surface, Physica E 73 (2015) 45–53.

[21] L.J. Crane, Flow past a stretching plate, Z. Angew. Math. Phys. 21 (4) (1970) 645–647.

[22] C.Y. Wang, Stretching a surface in a rotating fluid, Zeitschrift für angewandte mathematik und physic 39 (2) (1988) 177–185.

[23] H.S. Takhar, G. Nath, Unsteady flow over a stretching surface with a magnetic field in a rotating fluid, Zeitschrift für angewandte mathematik und physic 49 (6) (1998) 989–1001.

[24] H.I. Andersson, Slip flow past a stretching surface, Acta Mech. 158 (1-2) (2002) 121–125.

[25] R. Nazar, N. Amin, I. Pop, Unsteady boundary layer flow due to a stretching surface in a rotating fluid, Mech. Res. Comm.s, 31(2004), 8-121.

[26] E. Eldahab, M. Aziz, Blowing/suction effect on hydromagnetic heat transfer by mixed convection from an inclined continuously stretching surface with internal heat generation/absorption, Int. J. Ther. Sci. 43 (2004) 19–709.

[27] M. Kumari, T. Grosan, I. Pop, Rotating flow of power-law fluids over a stretching surface, J. Taiwan Insti. Chem. Eng. 26 (2006) 11–19.

[28] K. Govardhan, B. Balaswamy, N. Kishan, Unsteady boundary layer flow due to a stretching porous surface in a rotating fluid, Eng. Mech. 21 (2014) 269–277.

[29] M.W. Alam, S. Bhattacharyya, B. Souayeh, K. Dey, F. Hammami, M. Rahimi-Gorji, R. Biswas, Biswas CPU heat sink cooling by triangular shape micro-pin-fin: Numerical study, Int. Commun. Heat Mass Transfer 112 (2020) 104455, https://doi.org/10.1016/j.icheatmasstransfer.2019.104455.

[30] K.G. Kumar, A. Baslem, B.C. Prasannakumara, J. Majdoubi, M. Rahimi-Gorji, S. Nadeem, Significance of Arrhenius activation energy in flow and heat transfer of tangent hyperbolic fluid with zero mass flux condition. Microsystem Technologies. (2020) Aug;26(8):251726.

[31] S.C. Saha, M.S. Islam, M. Rahimi-Gorji, M.M. Molla, Aerosol particle transport and deposition in a CT-scan based mouth-throat model. InAIP conference proceedings (2019) Jul 18 (Vol. 2121, No. 1, p. 040011). AIP Publishing LLC.

[32] A. Zeeshan, Z. Ali, M.R. Gorji, F. Hussain, S. Nadeem, Flow analysis of biconvective heat and mass transfer of two-dimensional couple stress fluid over a paraboloid of revolution, Int. J. Mod. Phys. B 34 (11) (2020) 2050110, https://doi.org/10.1142/S0217979220501106.

[33] A. Bit, A. Alblawi, H. Chattopadhyay, Q.A. Quais, A.C. Benim, M. Rahimi-Gorji, H.T. Do, Three dimensional numerical analysis of hemodynamic of stenosed artery considering realistic outlet boundary conditions. Comput. Methods Programs Biomed. (2020) Mar 1;185:105163.

[34] I.-C. Liu, H.-H. Wang, Y.-F. Peng, Flow and heat transfer for three-dimensional flow over an exponentially stretching surface, Chem. Eng. Commun. 200 (2) (2013) 253–268.

[35] R. Kandasamy, N.A. bt Adnan, R. Mohammad, Nano-particle shape effects on squeezed MHD flow of water based Cu, Al2O3 and SWCNTs over a porous sensor surface, Alex. Eng. J., (2017), In press.

[36] E. Babolian, F. Fattahzadeh, Numerical solution of differential equations by using Chebyshev wavelet operational matrix of integration, App. Math., Comput. 188 (1) (2007) 417–426.

[37] F. Mohammadi, M.M. Hosseini, S.T. Mohyud-Din, Legendre wavelet galerkin method for solving ordinary differential equations with non-analytic solution, Int. J. Sys. Sci. 42 (4) (2011) 579–585.

[38] E. Magyari, B. Keller, Heat and mass transfer in the boundary layers on an exponentially stretching continuous surface, J. Phys. D: Appl. Phys., 32 (1999), 577–585.

[39] M. Fallah Najafabadi, H. Talebi Rostami, K. Hosseinzadeh, D. Domiri Ganji, Thermal analysis of a moving fin using the radial basis function approximation, Heat Transfer.

[40] K. Hosseinzadeh, M.R. Mardani, S. Salehi, M. Paikar, M. Waqas, D.D. Ganji, Entropy generation of three-dimensional Bödewadt flow of water and hexanol base fluid suspended by Fe_3O_4 and MoS_2 hybrid nano-particles, Pramana 95 (2) (2021 Jun) 1–4.

[41] K.h. Hosseinzadeh, S.o. Roghani, A.R. Mogharrebi, A. Asadi, M. Waqas, D.D. Ganji, Investigation of cross-fluid flow containing motile gyrotactic microorganisms and nano-particles over a three-dimensional cylinder, Alexandria Eng. J. 59 (5) (2020) 3297–3307.

[42] K.h. Hosseinzadeh, S. Salehi, M.R. Mardani, F.Y. Mahmoudi, M. Waqas, D.D. Ganji, Investigation of nano-Bioconvective fluid motile microorganism and nano-particle flow by considering MHD and thermal radiation, Inf. Med. Unlocked 21 (2020) 100462, https://doi.org/10.1016/j.imu.2020.100462.

[43] A.R. Mogharrebi, A.R. D. Ganji, K. Hosseinzadeh, S.o. Roghani, A. Asadi, A. Fazlollahtabar, Investigation of magnetohydrodynamic nano-fluid flow contain motile oxytactic microorganisms over rotating cone, Int. J. Numer. Meth. Heat Fluid Flow ahead-of-print (ahead-of-print) (2021), https://doi.org/10.1108/HFF-08-2020-0493.

[44] K.h. Hosseinzadeh, S.o. Roghani, A.R. Mogharrebi, A. Asadi, D.D. Ganji, Optimization of hybrid nano-particles with mixture fluid flow in an octagonal porous medium by effect of radiation and magnetic field, J. Therm. Anal. Calorim. 143 (2) (2021) 1413–1424.

[45] K.h. Hosseinzadeh, A. Asadi, A.R. Mogharrebi, M. Ermia Azari, D.D. Ganji, Investigation of mixture fluid suspended by hybrid nano-particles over vertical cylinder by considering shape factor effect, J. Therm. Anal. Calorim. 143 (2) (2021) 1081–1095.

[46] K.h. Hosseinzadeh, E. Montazer, M.B. Shafii, D.D. Ganji, Heat transfer hybrid nano-fluid (1-Butanol/MoS2–Fe3O4) through a wavy porous cavity and its optimization, Int. J. Numer. Meth. Heat Fluid Flow 31 (5) (2021) 1547–1567.

[47] S. Salehi, A. Nori, K.h. Hosseinzadeh, D.D. Ganji, Hydrothermal analysis of MHD squeezing mixture fluid suspended by hybrid nano-particles between two parallel plates, Case Studies Therm. Eng. 21 (2020) 100650, https://doi.org/10.1016/j.csite.2020.100650.

[48] M. Gholinia, K.h. Hosseinzadeh, D.D. Ganji, Investigation of different base fluids suspend by CNTs hybrid nano-particle over a vertical circular cylinder with sinusoidal radius, Case Studies Therm. Eng. 21 (2020) 100666, https://doi.org/10.1016/j.csite.2020.100666.